Measurement of K fluorescence yields of niobium and rhodium using monochromatic radiation

Jonathan Riffaud, Marie-Christine Lépy, Yves Ménesguen, A. Novikova

Special issue article

X-RAY SPECTROMETRY

Received: 15 September 2016 Revised: 22 December 2016 Accepted: 24 January 2017 Published online in Wiley Online Library: 15 March 2017

(wileyonlinelibrary.com) DOI 10.1002/xrs.2757

Measurement of K fluorescence yields of niobium and rhodium using monochromatic radiation

Jonathan Riffaud,* Marie-Christine Lépy, Yves Ménesguen and Anastasiia Novikova

Both reactions Nb-93(n,n′)Nb-93 m and Rh-103(n,n′)Rh-103 m are of particular importance for dosimetry in reactor, and the measurement of the activity of Nb and Rh dosimeters provides the basic data that can be traced back to the reactor operating information. These radionuclides emit only X-rays of which emission intensities in recommended data are determined thanks to the γ-ray transition probabilities and fluorescence yield values. In general, the knowledge of fluorescence yields is rather poor and based on old measurements. Nowadays, the use of tunable monochromatic X-ray sources allows performing optimized measurements. In a first step, accurate values of the attenuation coefficients are measured at the metrology beam line of the SOLEIL synchrotron, using procedures such as optimized for similar measurements. In a second step, the fluorescence yields are determined using experimental approaches in a traditional experimental configuration. For both materials, several incident energies are used to get experimental spectra with energy-dispersive spectrometer. The peaks of interest are processed using the COLEGRAM software, which allows detailed fitting of the peak shape. The K fluorescence yields are derived with about 2% relative uncertainty. Copyright © 2017 John Wiley & Sons, Ltd.

Keywords: K fluorescence yields; niobium; rhodium; synchrotron radiation

Introduction

For dosimetry of nuclear reactor, small metal samples are irradiated and activated by neutrons in the reactor core. After irradiation, the radioactivity of the samples is measured by conventional photon spectrometry. From the activity value and irradiation information, it is possible to determine the neutron flux at the dosimeter location. This technique allows characterizing the flux and the energy distribution of neutrons, validating neutrons codes and assessing reactor vessel aging. There are many dosimeters each characterizing a specific neutron energy region. For example, gold dosimeters are activated by radiative capture reaction, ^{197}Au(n,γ)^{198}Au and provide information on thermal neutrons, or iron dosimeters give information on fast neutrons with the energy around 3.1 MeV thanks to the reaction ^{54}Fe(n,p)^{54}Mn.

Inelastic scattering reactions (n,n′) are useful to characterize the neutron beams with energy around 1 MeV.[1–4] Both reactions ^{93}Nb(n,n′)^{93m}Nb and ^{103}Rh(n,n′)^{103m}Rh are of particular importance, and the activities of niobium and rhodium dosimeters are the basic data that can allow tracing back the reactor operating information. The activity of these dosimeters is measured by X-ray spectrometry[3,4], using spectrometers equipped with high purity germanium detectors, because ^{93m}Nb[5] and ^{103m}Rh[6] are radionuclides which emit only X-rays (Figs 1 and 2). Emission intensities of these X-rays in the recommended data[7] are determined from the γ-ray transition probabilities, internal conversion coefficients and fluorescence yield values. But, the knowledge of fluorescence yields is rather poor and based on old experiments. Indeed, there are some discrepancies between commonly used tables, and more experimental work is required to state which approach should be preferably used.[8]

Thus, it was decided to perform new measurements of the K fluorescence yields of niobium and rhodium taking advantage of optimized experimental facilities, using tunable monochromatic X-rays. The experiment included two steps: First, accurate values of the attenuation coefficients of niobium and rhodium were measured at the SOLEIL synchrotron,[9] using procedures such as optimized for similar measurements.[10,11] In a second step, the fluorescence yields were determined in a traditional experimental configuration where the target is installed at 45° both from the incident radiation and from an energy-dispersive detector.[12]

Experimental procedure

Most of the experiments were conducted at the Metrology beam line of the SOLEIL synchrotron facility (proposal 20160731). The hard X-ray branch is equipped with a double crystal monochromator (Si 111), providing monochromatic radiation with energies in the 3.5 to 35-keV range. It is important to have an accurate energy calibration of the resulting photons. The link between the

* Correspondence to: Jonathan Riffaud, CEA, LIST, Laboratoire National Henri Becquerel (LNE-LNHB), CEA-Saclay, 91191 Gif-sur-Yvette Cedex, France. E-mail: jonathan.riffaud@cea.fr

Presented at EXRS2016 - European Conference on X-ray Spectrometry, Gothenburg, Sweden, 19–24 June 2016.

CEA, LIST, Laboratoire National Henri Becquerel (LNE-LNHB), CEA-Saclay, 91191, Gif-sur-Yvette Cedex, France

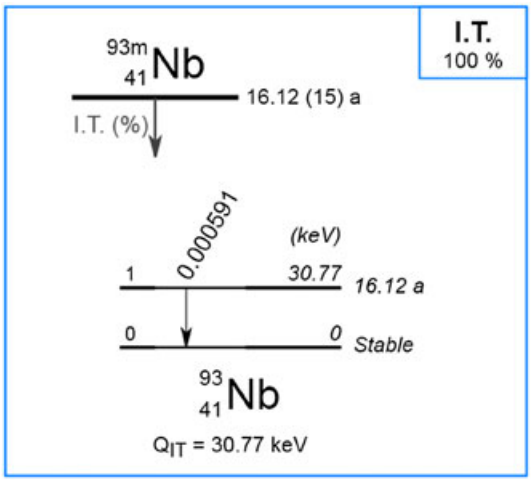

Figure 1. Decay scheme of ^{93m}N[7].

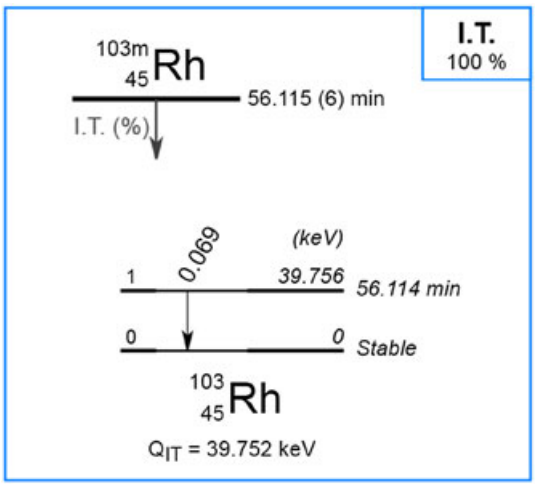

Figure 2. Decay scheme of ^{103m}Rh[7].

monochromator angle and the energy of the photons E is established with an associated uncertainty of $10^{-5}E$. The relative photon flux intensity stability is better than 0.3% due to the top-up mode of the synchrotron, and high-order harmonics are rejected by a small detuning of the second crystal (necessary only for energies below 7 keV).

The samples used for the measurements have purity higher than 99.994% for niobium and 99.97% for rhodium, certified by the Institute for Reference Materials and Measurements.

Mass attenuation coefficients

Before measuring the fluorescence yields, it is necessary to get accurate values of mass attenuation coefficients of niobium and rhodium. These coefficients were obtained following an experimental procedure previously established and validated for similar measurements on germanium, copper and other metallic targets.[10–12] Mass attenuation coefficients, $\frac{\mu}{\rho}(E)$, were measured in transmission mode using a monochromatic parallel photon beam with energy E under normal incidence to the sample with thickness x. The principle of the measurement consists in measuring the intensity of photon flux before the sample, $I_0(E)$, and immediately after it $I(E)$. For a monochromatic photon beam, the attenuation follows the Beer–Lambert law:

$$\mathbf{I} = \mathbf{I}_0\, \mathbf{e}^{-\frac{\mu}{\rho}(\mathbf{E})\rho\mathbf{x}} = \mathbf{I}_0 \mathbf{e}^{-\frac{\mu}{\rho}(\mathbf{E})\frac{\mathbf{M}}{\mathbf{A}}} \quad (1)$$

where μ is the linear attenuation coefficient of the target material and ρ is the material density.

Direct measurement of thickness of a few micrometres with an uncertainty lower than 1% was not possible. On the other side, it was easier to perform a measurement of the mass per unit area $\frac{M}{A}$ of the target (where M is the target mass and A its area) with lower uncertainty. The mass was measured thanks to a precision microbalance and the surface area using a vision machine associated with a dedicated pictures processing software. The mass of the samples are measured with a relative uncertainty of 0.04% for niobium and 0.02% for rhodium, and the area is known with a relative uncertainty of 0.04% for niobium and 0.05% for rhodium. The intensities $I(E)$ and $I_0(E)$ are measured at a single point behind the sample, with and without the sample, respectively. Special care was taken around the K binding energies of niobium and rhodium and on the energy of their characteristic X-rays, because these values are directly used in the next step, for the determination of the fluorescence yields. Although the mass attenuation coefficients below the K binding energy are not required for the fluorescence experiment, the measurement was carried out on a large energy range. This was stated in order to compare the experimental results with tabulated values on a large scale. In addition, the difference between the coefficients values on each side of the K edge allows assessing the target thickness.

The mass attenuation coefficient is presented as a function of the energy in Figs 3 and 4 for niobium and rhodium in the energy ranges between 7 and 35 keV and 17–35 keV, respectively. The relative combined standard uncertainties computed from elemental uncertainties on I, I_0 and $\frac{M}{A}$ are around 2%. The results obtained during these measurements are compared to the values of XCOM[13] and CXRO[14] that can be easily obtained through a website. The first one is a compilation of experimental and theoretical works, based on Scofield[15] calculations using a Hartree–Slater atomic model. The second focusses on the energy range lower than 30 keV and is a semi-empirical approach, including theory based on atomic scattering factors. The graphs show a difference between databases and the measured values here for energies above the K binding energy where these values are larger of a few percent.

Fluorescence yields

The experimental setup for measuring fluorescence yields is presented in Fig. 5. The target (niobium or rhodium) is placed in the path of a monochromatic photon beam, with energy E_0 and intensity I_0, α being the incidence angle. The beam is attenuated according to the linear attenuation coefficient $\mu_0 = \mu(E_0)$ and interacts with the target material at depth x by photoelectric effect in the K shell with the probability τ_K. Following the electronic rearrangement, X-rays are emitted with energy E_i according to the partial K fluorescence yield ω_{Ki}. The attenuation of the fluorescence radiation in the target material depends on the attenuation coefficient at the energy of the fluorescence radiation $\mu_i = \mu(E_i)$. These photons are measured under the emission angle β, in an elemental solid angle, $d\Omega$, by a high purity germanium detector.

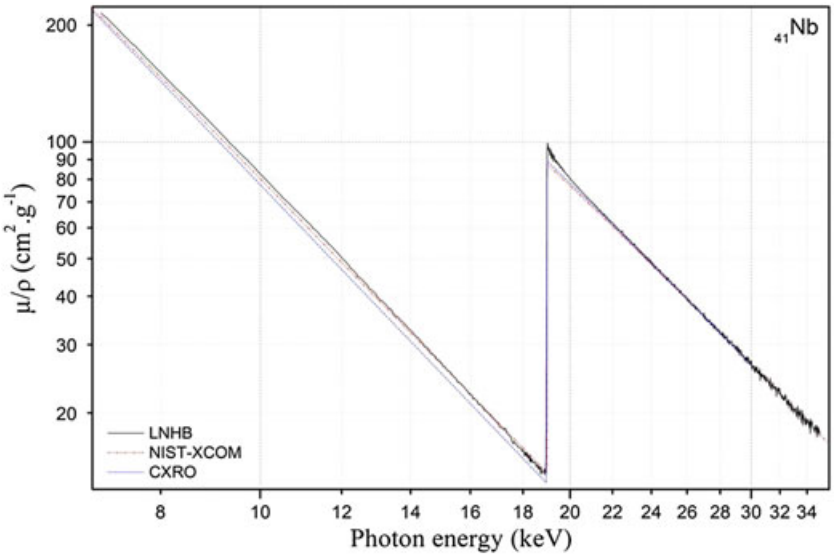

Figure 3. Niobium mass attenuation coefficients *versus* the energy.

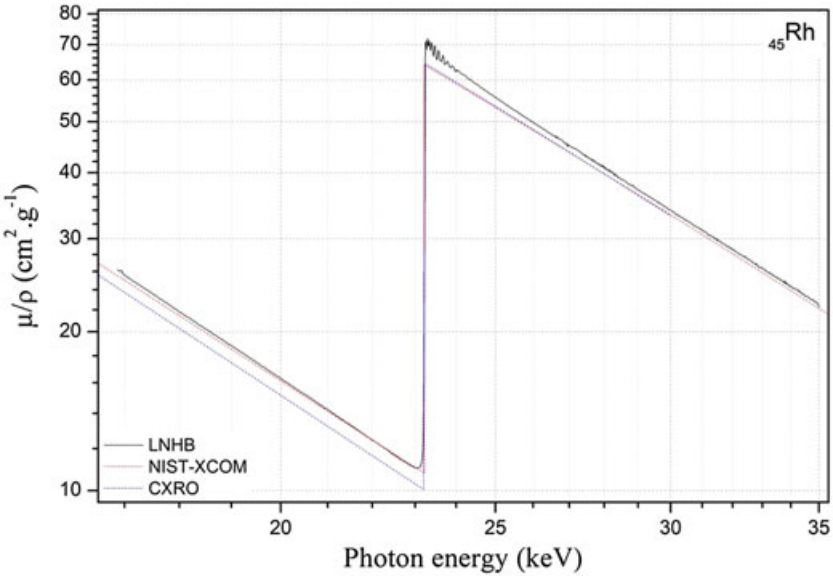

Figure 4. Rhodium mass attenuation coefficients *versus* the energy.

The full-energy peak efficiency ε_i of the detector was previously established with about 1% relative uncertainty.[16] Thus, dN_i, the elemental number of events consecutive to an interaction in the elemental thickness dx and recorded in the full-energy peak, results from:

i Absorption of the incident photon beam in the target material elemental thickness *dx* at depth *x*: $I_0\, e^{-\frac{\mu_0 x}{\sin\alpha}}\, \frac{dx}{\sin\alpha}$
ii Interaction by photoelectric effect in the K shell: τ_K
iii Atomic relaxation by X-ray emission: ω_{Ki}
iv Absorption of the emitted fluorescence radiation within the target material: $e^{-\frac{\mu_i x}{\sin\beta}}$
v Emission of the fluorescence radiation in the elemental solid angle of detection: $\frac{d\Omega}{4\pi}$
vi Interaction and deposition of the full energy of the fluorescence radiation in the detector: ε_i

$$dN_i = I_0\, e^{-\frac{\mu_0 x}{\sin\alpha}}\, \tau_K \frac{dx}{\sin\alpha}\, \omega_{Ki}\, e^{-\frac{\mu_i x}{\sin\beta}} \frac{d\Omega}{4\pi}\, \varepsilon_i \qquad (2)$$

Here, the target is placed at the angle of 45° relative to the incident beam; thus, $\alpha = \beta$, what simplifies Eqn (2). By integrating this equation on the target thickness and the solid angle, we can deduce the partial K fluorescence yield:

$$\omega_{Ki} = \frac{4\pi}{\Omega} \frac{N_i}{\varepsilon_i} \frac{1}{I_0 \tau_K} \frac{\mu_0 + \mu_i}{1 - e^{-\frac{\mu_0 + \mu_i}{\sin\frac{\pi}{4}} l}} \qquad (3)$$

The photodiode placed behind the target measures the current induced by the transmitted beam, C_t. The photodiode efficiency (*A/keV*), ε_{Pi}, was absolutely calibrated using a cryogenic electrical-substitution radiometer.[17] The target transmission at 45° can be derived from the target mass par unit area, measured as described above, and mass attenuation coefficients previously established:

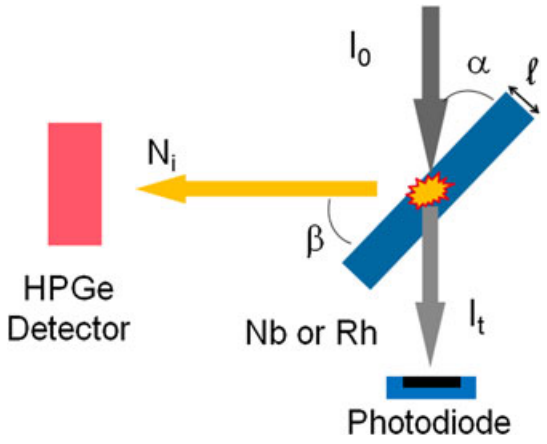

Figure 5. Geometry of the experimental setup for fluorescence yield measurements.

$$T_i = e^{\left(\frac{\mu_{(E)}}{\rho}\times\frac{M}{A}\right)} \quad (4)$$

For each energy E_i, the intensity I_0 of the incident photon beam is thus obtained as

$$I_O = C_t \times \varepsilon_{Pi} \times E_i \times T_i \quad (5)$$

Results and discussion

The measurements were performed with nominal thickness of niobium and rhodium targets 20 and 50 μm, respectively (measured mass per unit area are 0.017042 (10) g cm^{-2} for Nb and 0.058962 (32) g cm^{-2} for Rh). Several incident energies were used to get several results and consequently guarantying these experimental values and associated uncertainties, because in the different experiments, some parameters (attenuation coefficients,

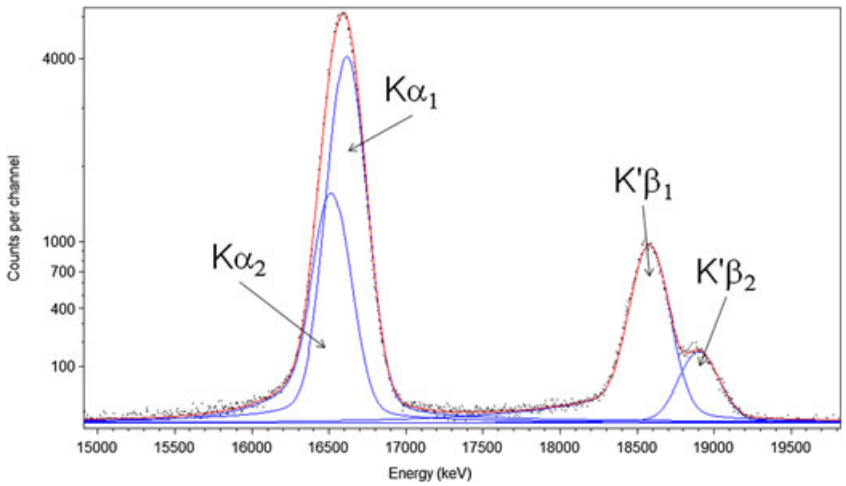

Figure 6. Processing of the niobium K X-rays region using COLEGRAM sofware.

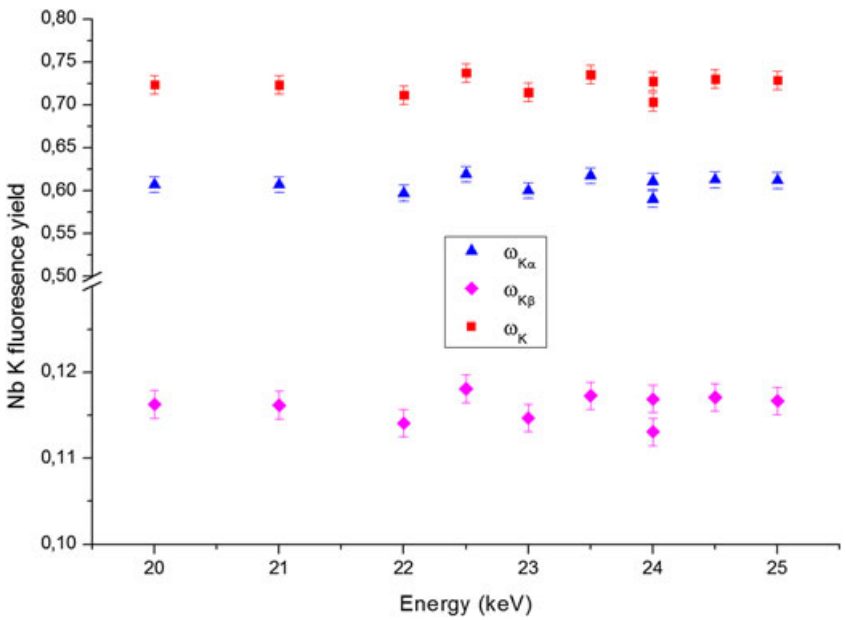

Figure 7. Niobium partial and total K fluorescence yields obtained with different incident energies.

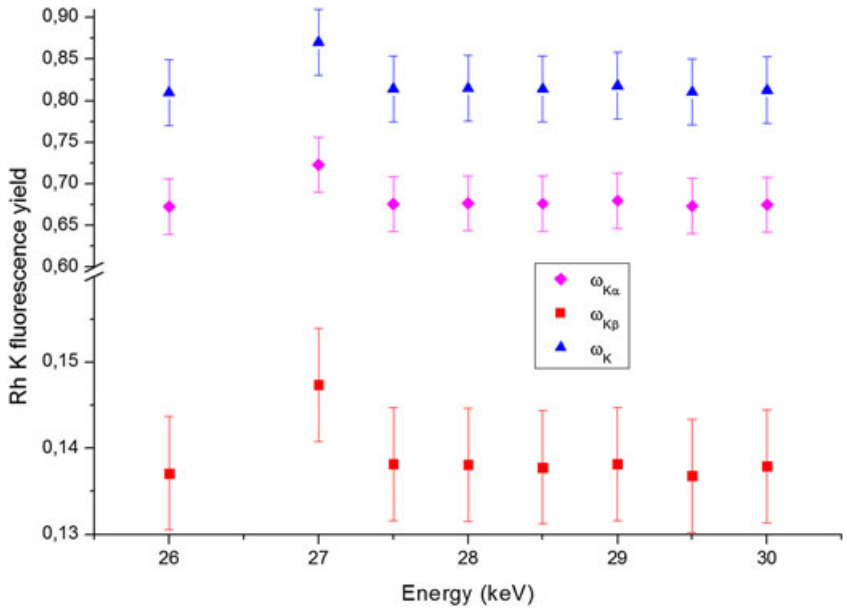

Figure 8. Rhodium partial and total K fluorescence yields obtained with different incident energies.

Table 1. : K fluorescence yield values for niobium

—	Experimental	Theoretical	Semi-empirical
Present work	0.724 (14)	—	—
Roos[21,22]	0.713	—	—
	0.730 (20)	—	—
Callan[23]	—	0.754	—
Kostroun[24]	—	0.759	—
Walters *et al.*[25]	—	0.7788	—
Bambynek *et al.*[26]	—	—	0.748 (32)
Krause[27]	—	—	0.747
Arora *et al.*[28]	0.738 (30)	—	—
Hubbell *et al.*[29]	—	—	0.7512
Singh *et al.*[20,32]*	0.722 (44)	—	—
Hubbell *et al.*[20]	—	—	0.724
Schönfeld *et al.*[30]	—	—	0.751 (4)
Durak *et al.*[31]	0.734 (28)	—	—
Han *et al.*[19]	0.747 (60)	—	—
Kahoul *et al.*[32]	—	—	0.73993

Table 2. K fluorescence yield values for rhodium

—	Experimental	Theoretical	Semi-empirical
Present work	0.814 (41)	—	—
Backhurst[33]	0.801	—	—
Stephenson[34]	0.77	—	—
Roos[21,22]	0.779	—	—
	0.786 (15)	—	—
Callan[23]	—	0.812	—
Kostroun[24]	—	0.820	—
Walters *et al.*[25]	—	0.8367	—
Bambynek *et al.*[26]	—	—	0.807 (31)
Krause[27]	—	—	0.808
Chen *et al.*[35]	—	0.808	—
Hubbell[29]	—	—	0.8086
Singh *et al.*[20,32]*	0.829 (58)	—	—
Hubbell *et al.*[20]	—	—	0.792
Schönfeld *et al.*[30]	—	—	0.809 (4)
Kahoul *et al.*[32]	—	—	0.80205

photodiode and energy-dispersive detector efficiencies, etc.) change; thus, a constant final result means that the experimental conditions are well controlled. For niobium, results were obtained on the average of 10 measurements with incident photons in the 20 to 25-keV energy. Spectra obtained after the acquisition were treated with the COLEGRAM processing software[18] dedicated to spectrometry to fit the results with different functions depending on the nature of the particle (X- or γ- photon, alpha, etc.). A spectrum processing example for the niobium is shown in Fig. 6. Peaks from X-rays are fitted with Voigt function, convolution of a Gaussian function and a Lorentzian function. The Gaussian broadening corresponds mainly to the statistic of electron–hole pair creation in germanium, while the Lorentzian broadening is due to the natural linewidth of X-rays.

Figure 7 shows the results of these measurements, including partial Kα and Kβ and total K fluorescence yields of niobium. The average value of the total K fluorescence yield niobium obtained is ω_K = 0.724 (14). For rhodium, results were obtained with an average of eight measurements with incident photons in the 26 to 30-keV energy range. The partial Kα and Kβ and total K fluorescence yields of rhodium resulting from these measurements are presented in Fig. 8. The average value of the total K fluorescence yield rhodium obtained is ω_K = 0.814 (41).

The relative standard uncertainties of the measurements are about 2% for niobium and 5% for rhodium. The difference between these is explained by larger uncertainties on intensity measurements of the photon flux for the rhodium. Indeed, the rhodium target is thicker and significantly reduces the initial beam intensity. Thus, the transmitted intensity values measured by the photodiode

are closer to the background noise value than niobium, which increases the uncertainty on rhodium measurements.

Tables 1 and 2 show the experimental values for niobium and rhodium obtained in this work and the comparison them with other values, experimental, theoretical or semi-empirical. First, one can see a limited number of recent experimental values. There are only six experimental values for Nb, with relative differences up to 4%. The associated uncertainties, when quoted, are between 3 and 8%. There are five experimental values for Rh, which was measured only once over the last 60 years, with relative differences of 8%. Only the Ross[21] value (60-year-old measurement) quotes relative uncertainties of 2%. Second, there is a significant difference between the experimental and theoretical values, mainly for niobium (about 4%).

The niobium fluorescence yield presently determined is in agreement with the other experimental results, except the one measured by Han[19]. It is also very close to the value quoted by Hubbell[20] obtained from a fit of experimental values.

For rhodium, the measured value is higher than most of the other experimental values. However, it is quite close to the value measured by Singh[20,32][1] and in agreement with the theoretical values, except the one computed by Walters.[23]

Conclusion

Recent experimental, theoretical or semi-empirical data of K fluorescence yield for niobium and rhodium are uncommon. Moreover, the differences in results between each method are pretty important. In this work, we measured the niobium and rhodium fluorescence yield using a new tunable source delivering monochromatic photons, which present an unprecedented quality and allow the development of new experimental protocols of fundamental parameter measurement. It also allows obtaining fluorescence yield values with assessed uncertainty on the measurement result. The uncertainty is clearly improved for niobium (2% relative uncertainty compared to 3 to 8% for the other experimental data). For rhodium, the target was too thick to get results with low uncertainty. New measurements of rhodium fluorescence yield with thinner sample are planned to reduce this uncertainty. It is expected that the results obtained in this study will contribute to establishing a benchmark for the Nb and Rh K fluorescence yield values. This should lead to an improved knowledge of the X-ray emission probabilities useful for accurate neutron dosimetry and other applications.

Acknowledgments

We acknowledge SOLEIL for the provision of synchrotron radiation facilities with special thanks to Paulo da Silva and Pascal Mercere for assistance in using the 'Metrologie' beamline.

References

[1] A. Ballesteros, L. Debarberis, W. Voorbraak, J. Wagemans, P. D'hondt. *Prog Nucl Energy* **2010**, *52*, 615–619.
[2] W. P. Voorbraak, T. Kekki, T. Serén, M. van Boxstaele, J. Wagemans, J. R. W. Woittiez, Proceeding of the FISA-2003 conference **2003**, https://cordis.europa.eu/fp5-euratom/src/ev-fisa2003.htm, [Accessed on 2016]
[3] V. Sergeyeva, C. Domergue, C. Destouches, J.-M. Girard, H. Philibert, D. Beretz, J. Bonora, N. Thiollay, A. Lyoussi, Eur. Phys. J. Web of conference **2016**; *106*, 05011. DOI: 10.1051/epjconf/201610605011
[4] C. Domergue, D. Beretz, C. Destouches, J. M. Girard, H. Philibert, J. Plagnard, Advancements in nuclear instrumentation measurement methods and their applications (ANIMMA), 2009 First International Conference on, Marseille **2009**, pp. 1–6. DOI: 10.1109/ANIMMA.2009.5503820
[5] M.-M. Bé, V. Chisté, C. Dulieu, M.A. Kellett, X. Mougeot, A. Arinc, V.P. Chechev, N.K. Kuzmenko, T. Kibédi, A. Luca, A.L. Nichols. Table of radionuclides, Monographie BIPM-5 8 (BIPM, Pavillon de Breteuil, F-92310 Sèvres, France, **2016**).
[6] Private communication. M.-M. Bé, M.A. Kellett **2016**.
[7] Nucleide **2016**, http://www.nucleide.org/DDEP_WG/DDEPdata.htm, [Accessed on 2016]
[8] J. L. Campbell. *IRPS Bulletin* **2010**, *24*(1), 17–30.
[9] SOLEIL synchrotron, http://www.synchrotron-soleil.fr/portal/page/portal/Accueil, [Accessed on 2016]
[10] Y. Ménesguen, M.-C. Lépy. *Nuc Instrum Methods Phys Res, Sect B* **2010**, *268*, 2477–2486.
[11] Y. Ménesguen, M. Gerlach, B. Pollakowski, R. Unterumsberger, M. Haschke, B. Beckhoff, M.-C. Lépy. *Metrologia* **2016**, *53*, 7–17.
[12] J. M. Sampaio, T. I. Madeira, J. P. Marques, F. Parente, A. M. Costa, P. Indelicato, J. P. Santos, M.-C. Lépy, Y. Ménesguen. *Phys Rev A* **2014**, *89*, 012512.
[13] XCOM, http://www.physics.nist.gov/PhysRefData/Xcom/html/xcom1.html, [Accessed on 2016]
[14] B. L. Henke, E. M. Gullikson, J. C. Davis. *Atom Data Nucl Data Tables* **1993**, *54*, 181–342.
[15] J.H. Scofield, Lawrence Livermore National Laboratory report UCRL-51326, **1973**.
[16] J. Plagnard, C. Bobin, M.-C. Lépy. *X-Ray Spectrom.* **2007**, *36*, 191–198.
[17] P. Troussel, N. Coron. *Nuc. Instrum. Methods Phys. Res., Sect. A* **2010**, *614*, 260–270.
[18] H. Ruellan, M.-C. Lépy, M. Etcheverry, J. Plagnard, J. Morel. *Nuc Instrum Methods Phys Res, Sect A* **1996**, *369*, 651–656.
[19] I. Han, M. Sahin, L. Demir, Y. Sahin. *Appl Radiat Isot* **2007**, *65*, 669–675.
[20] J. H. Hubbell, P. N. Trehan, N. Singh, B. Chand, D. Mehta, M. L. Garg, R. R. Garg, S. Singh, S. Puri. *J. Phys. Chem. Ref. Data* **1994**, *23*, 339–363.
[21] C. E. Roos. *Phys. Rev.* **1954**, *93*, 401–405.
[22] C. E. Roos. *Phys. Rev.* **1957**, *105*, 931–935.
[23] E. J. Callan*Role of Atomic Electrons in Nuclear Transformations*, Nuclear Energy Information Center, Warsaw, **1963**.
[24] V. O. Kostroun. *Phys Rev A* **1971**, *3*, 533–545.
[25] D. L. Walters, C. P. Bhalla. *Phys Rev* **1971**, *3*, 1919–1927.
[26] W. Bambynek, B. Crasemann, R. W. Fink, H.-U. Freund, H. Mark, C. D. Swift, R. E. Price, P. Venugopala Rao. *Rev Mod Phys* **1972**, *44*, 716–813.
[27] M. O. Krause. *J Phys Chem Ref Data* **1979**, *8*, 307–327.
[28] S. K. Arora, K. L. Allawadhi, B. S. Sood. *Physica B + C (Amsterdam)* **1981**, *111*, 71–75.
[29] J. H. Hubbell, NISTIR **1989**, 89–4144.
[30] E. Schönfeld, H. Janßen. *Nuc. Instrum. Methods Phys. Res., Sect. A* **1996**, *369*, 527–533.
[31] R. Durak, Y. Özdemir. *Radiat Phys Chem* **2001**, *61*, 19–25.
[32] A. Kahoul, A. Abassi, B. Deghfel, M. Nekkab. *Radiat. Phys. Chem.* **2011**, *80*, 369–377.
[33] I. Backhurst. *Philosoph Mag* **1936**, *22*, 737–752.
[34] R. J. Stephenson. *Phys. Rev.* **1937**, *51*, 637–642.
[35] M. H. Chen, B. Crasemann, H. Mark. *Phys Rev A* **1980**, *21*, 436–441.
[36] S. Singh, R. Rani, D. Mehta, N. Singh, P. C. Mangal, P. N. Trehan. *X-Ray Spectrom* **1990**, *19*, 155–158.

[1]The values cited in these references[20,32] come from the same article from Singh[36] that deals with another topic where these values do not appear.